ELSEVIER

Physica E 10 (2001) 45–51

PHYSICA E

www.elsevier.nl/locate/physe

Spin effects in semiconductor quantum dot structures

S. Tarucha[a,b,*], D.G. Austing[b], S. Sasaki[b], Y. Tokura[b], J.M. Elzerman[c], W. van der Wiel[c], S. de Franseschi[c], L.P. Kouwenhoven[c]

[a] *ERATO Mesoscopic Correlation Project, Department of Physics, University of Tokyo, 7-3-1, Hongo, Bunkyo-ku, Tokyo, 113-0033, Japan*

[b] *NTT Basic Research Laboratories, 3-1, Morinosato Wakamiya, Atsugi-shi, Kanagawa 243-0198, Japan*

[c] *ERATO Mesoscopic Correlation Project, Department of Applied Physics, Delft University of Technology, PO Box 5046, 2600 GA Delft, The Netherlands*

Abstract

The spin effects on the electronic properties are studied for two different quantum dots: a quantum dot well isolated from the leads and that strongly coupled to the leads. For the first quantum dot, we use a magnetic field to adjust the single-particle state degeneracy, and observe a singlet–triplet transition at zero and non-zero magnetic fields, favored by direct Coulomb and exchange interactions. The spin configurations in an arbitrary magnetic field are well explained in terms of two-interacting electron model. For the second quantum dot we adjust the single-particle state degeneracy as a function of magnetic field and observe a novel Kondo effect associated with the singlet–triplet degeneracy. This Kondo anomaly appears when the quantum dot holds an even number of electrons, and the characteristic energy scale is much larger than in the ordinary half-spin case.

PACS: 73.23.Hk; 73.20.Dx; 72.15.Qm; 71.70.Gm

Keywords: Artificial atom; Quantum dots; Spin effect; Kondo effect; Exchange interaction

1. Introduction

Adding electrons to a quantum dot costs extra energy associated with the quantum mechanical effect and interaction effect (for review, see Refs. [1–3]). The resulting electronic configuration in the dot is determined to minimize the total energy of the system. The spin state, thus determined, usually takes a total spin, $S = 0$ when the number, N, of electrons in the dot is even, and $S = \frac{1}{2}$ for odd N. S can be greater than $\frac{1}{2}$ when the spin-related interaction is strong. We have previously studied the

* Corresponding author. Department of Physics, University of Tokyo, 7-3-1, Hongo, Bunkyo-ku, Tokyo 113-0033, Japan. Tel.: +81-35841-4533; fax: +81-35841-4162.

E-mail address: tarucha@phys.s.u-tokyo.ac.jp (S. Tarucha).

1386-9477/01/$ - see front matter
PII: S1386-9477(01)00051-0

electronic configurations in a vertical quantum dot, and found that the spin state is determined in line with Hund's first rule for the shell filling [4,5]. This is the case for the filling of degenerate orbital states confined by two-dimensional (2D) harmonic potential, and the high-spin state is favored by exchange interaction.

In this paper we use a vertical quantum dot to study the spin effects for the simplest system, i.e., a state made out of two electrons. The spin state is then either a singlet or a triplet. We control over a transition between a spin singlet and a triplet by tuning the degeneracy of orbital states as a function of magnetic field, B. In our vertical quantum dot N is varied one-by-one, starting from 0, and the electronic states are well described using single-particle quantum numbers. The electronic states evolve with B-field in a systematic way. When the single-particle states in the dot are well separated, an antiparallel spin filling is favored. On the other hand, when the separation is small, parallel spin filling is favored in line with Hund's first rule. This allows us to alter the way of spin filling. We experimentally determine the contributions from direct Coulomb (DC) and exchange (EX) to Hund's first rule [6], using a quantum dot well isolated from the external leads. On the other hand, when a dot is strongly coupled to the external leads, Heisenberg uncertainty makes more significant the virtual tunneling process between the leads via the dot, i.e., the tunneling of the (uppermost) electron on the dot to one of the leads whereupon it is replaced quickly by another electron. This is called a co-tunneling process, and holds even when the energy level of uppermost electron is well bellow the Fermi energies of the two leads. At low temperature, the coherent superposition of all possible co-tunneling processes involving spin flip can result in a time-averaged spin equal to zero. The whole system forms a singlet, leading to "Kondo anomaly" [7,8], which is previously observed for quantum dots holding an odd number of electrons or a half-integer spin [9–12]. To study the spin effects in Kondo anomaly we prepare a vertical quantum dot having the tunnel resistance comparable to the quantum resistance. By tuning a singlet–triplet transition for a two-electron state, we find novel Kondo anomaly associated with degeneracy between a spin singlet and a triplet [13]. The obtained Kondo temperature is significantly higher than that for conventional Kondo anomaly.

2. Control over a two-electron spin state

2.1. Model for two interacting electrons

We first discuss a simple model that describes filling of two single-particle states with two interacting electrons. Fig. 1(a) shows two, spin-degenerate single-particle states with energies E_a and E_b crossing each other at $B = B_0$. The electrochemical potential, $\mu(1)$ (=total energy), of the ground state (GS) for one electron occupying these states, equals E_a for $B < B_0$ and E_b for $B > B_0$ (thick line in Fig. 1(a)). For two electrons we can distinguish four possible configurations with either $S = 0$ (spin-singlet) or $S = 1$ (spin-triplet). Here, we neglect the Zeeman energy. The corresponding electrochemical potential, $\mu_i(2)$, which is given by the difference in the total energy between one- and two-electron system, is schematically shown in Fig. 1(b). The GS is determined by the minimum in the electrochemical potential (bold line in Fig. 1(b)). The fine lines are all excited states (ES_s). The GS is a singlet, which has two antiparallel electrons in the state with E_a (μ_1) for $B < B_0$ and E_b (μ_2) for $B > B_0$. Near B_0, the GS is a triplet (μ_3) characterized by a downward cusp. This triplet has two parallel spins in each state of E_a and E_b. Parallel to and above this triplet there is a singlet (μ_4) having two electrons in the same orbitals as for the triplet. The excitation energy is given by $2|K_{ab}|$, where K_{ab} is EX energy. On both ends of the downward cusp there is a transition between a singlet and a triplet (labeled "S–T" and "T–S"). The difference in the electrochemical potential between the one and two electron systems outside the downward cups is equivalent to the DC energy, C_{ii} ($i = a, b$), between two electrons occupying the same state with E_i. If the states with E_a and E_b have the same type of orbitals, EX interactions only contribute to the downward cusp. This is typically the case for Hund's first rule in the second shell at $B = 0$ T, which is observed in the circular dot [4,5]. However, states at the crossings at finite fields usually have different types of orbitals, so both of EX and DC interactions can significantly contribute to the downward cusp.

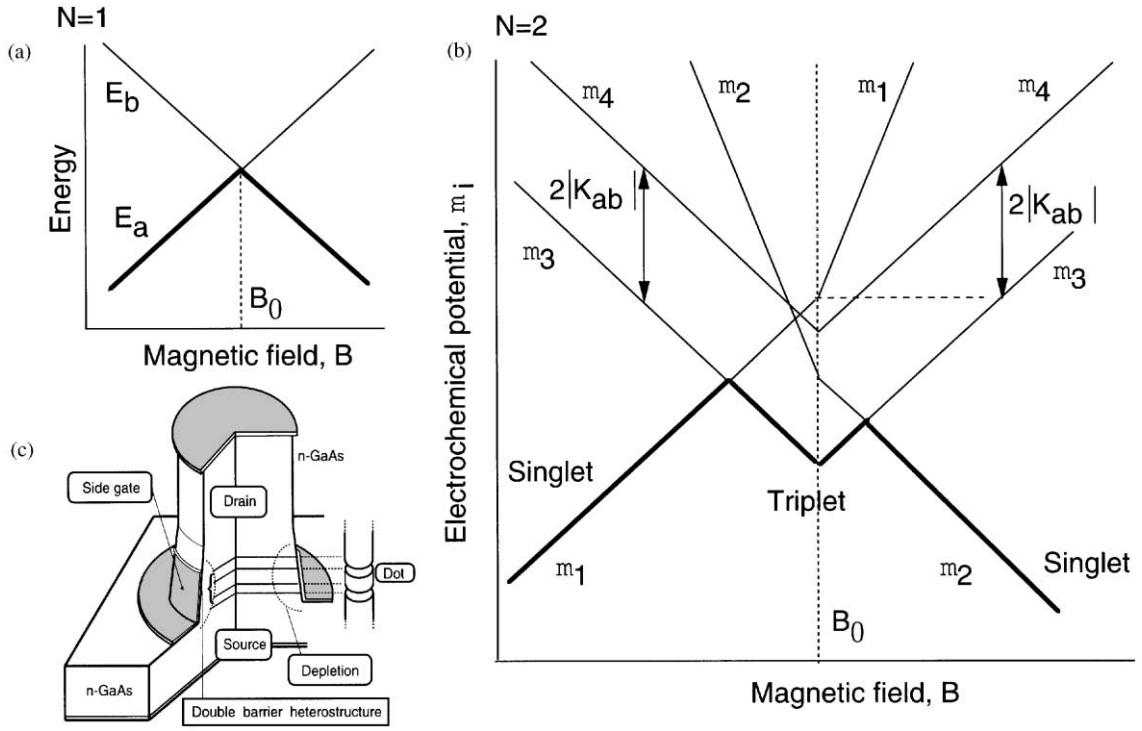

Fig. 1. (a) Schematic diagram of two single-particle states with energies E_a and E_b crossing each other at a magnetic field $B = B_0$. (b) Electrochemical potential, $\mu_i(2) = U_i(2) - U(1)$, for two interacting electrons. The thick line represents the ground state energy whereas the thin lines show the excited states. (c) Schematic diagram of a quantum dot in a vertical device. The quantum dot is located inside the 0.54 μm-diameter pillar.

2.2. Experimental

Our semiconductor quantum dot is located in a cylindrical mesa and has the shape of a 2D disk (see Fig. 1(c)). This quantum dot is coupled to the leads with the tunnel resistance much greater than the quantum resistance. We usually set the source–drain voltage, V, at a small value and observe series of current peaks (i.e. Coulomb peaks) corresponding to be a one-by-one change in N [1–3]. The position of a Coulomb peak for the transition from $N-1$ to N measures the GS electrochemical potential $\mu(N)$.

The eigenstates for a 2D harmonic potential (characteristic energy, $\hbar\omega_0$) in the presence of B-field parallel to the current are the Fock–Darwin (FD) states [14,15]. Fig. 2(a) shows the eigen energy vs. B calculated for $\hbar\omega_0 = 2$ meV. Spin splitting is neglected so each state is two-fold degenerate. The orbital degeneracy at $B = 0$ T is lifted on initially increasing B. As B is increased further, new crossings or new degeneracies can occur. The last crossing occurs along the bold line in Fig. 2(a). Each oval highlights the single crossing that we concentrate on for discussing the two-electron filling of two degenerate orbitals.

Fig. 2(b) shows the evolution of Coulomb peaks, i.e. the GS electrochemical potentials, with B-field for $N = 7$–16. Features associated with a 2D parabolic confining potential are all observed, such as pairing of neighboring peaks, and a shell structure [4,5]. Large peak spacings at $B = 0$ T are observed for $N = 2$, 6, 12 and 20. The large spacing for $N = 12$ can be seen in Fig. 2(b). These large spacings reflect the complete filling of the first four shells. The pairing between neighboring peaks indicates anti-parallel spin filling by two electrons in a single orbital state. The wiggles or anti-crossings between pairs of peaks correspond to the crossings of FD states. Modifications to the simple pairing of peaks are observed for the peaks

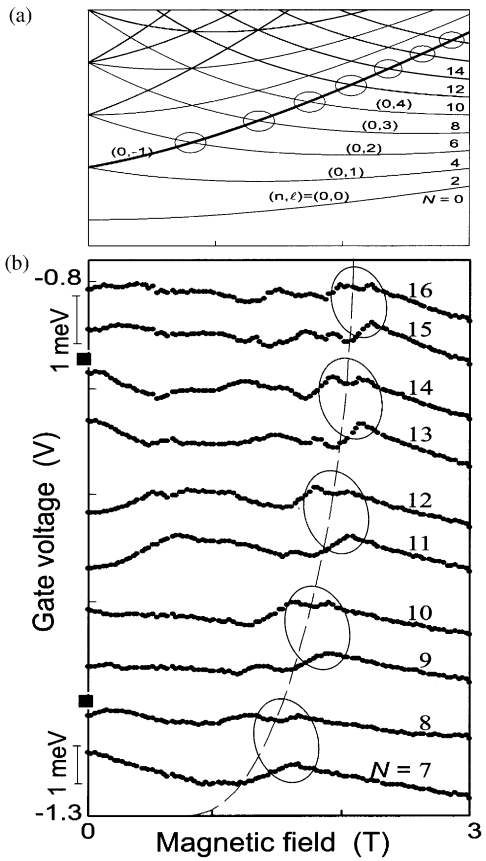

Fig. 2. (a) Fock–Darwin states calculated for $\hbar\omega_0 = 2$ meV. Dashed circles indicate the last crossing of the Fock–Darwin states. (b) B-field dependencies of current peak positions from $N = 7$ to 16. The bars along the gate voltage axis show 1 meV energy scales calibrated at -1.26 and -0.85 V. The long dashed curve indicates the last crossing between single-particle states. Dashed ovals group pairs of ground states for odd and even electron numbers. Spin transitions in the ground states are indicated by ■ at $B = 0$ T and occur inside the ovals for $B \neq 0$ T.

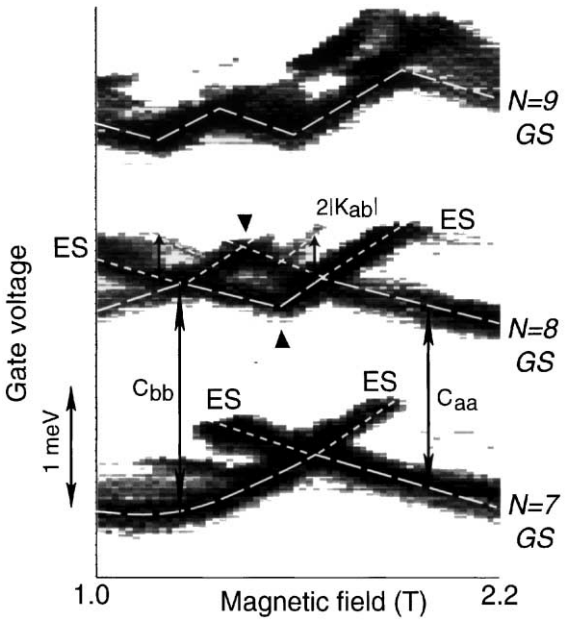

Fig. 3. dI/dV_g in the plane of V_g and B for $N = 7$–9 measured for $V = 0.84$ mV. $dI/dV_g > 0$ for dark and $dI/dV_g \leqslant 0$ for bright. The long dashed white lines indicate the evolution of the ground states with magnetic field whereas the dotted white lines show the excited states. The two arrows indicate singlet–triplet (S–T) and triplet–singlet (T–S) transitions in the ground state for $N = 8$.

labeled by ■ at 0 T, and in each dashed oval connecting pairs of peaks along the dashed line at non-zero field. ■ corresponds to the filling of the second electron in the third and fourth shells, respectively. Each oval indicates the two-electron filling at the crossing of two FD states marked by the oval in Fig. 2(a). As we substantiate below, these are all signatures of Hund's first rule.

More detailed agreement between experiment and the model for both the GSs and ESs are obtained by measuring the excitation spectrum [16]. Fig. 3 shows a derivative plot, dI/dV_g, taken for $V = 0.84$ mV. This larger voltage opens a sufficiently wide transport window between the Fermi levels of the source and drain such that both GS and ES can be detected. The GS and ESs for $N = 7$–9 are assigned from the dark lines. Long-dashed white lines highlight the GSs whereas the ESs are indicated by dotted white lines. The set of GS and ES lines for $N = 7$ shows a single crossing similar to Fig. 1(a). The spectrum for $N = 8$ compares well with Fig. 1(b) and we can clearly distinguish the parallelogram formed by the GS and first ES. The singlet–triplet transitions in the GS for $N = 8$ can also be identified and are indicated by arrows. Parallel to and above the triplet there appears an ES. This is a singlet having the same orbital configuration as the triplet, and the excitation energy is equivalent to $2|K_{ab}|$ (=0.25 meV). From the difference between the parallel GSs lines for $N = 7$ and 8 we evaluate $C_{aa} = 1.90$ meV and $C_{bb} = 1.46$ meV. All of these values of C_{aa}, C_{bb} and $|K_{ab}|$ compare well with the calculation. The downward cusp in the GS for $N = 8$

(labeled ▲) is at a slightly higher B-field than the upward cusp in the first ES (labeled ▼). This asymmetry implies that $C_{aa} > C_{bb}$. The same type of asymmetry is always observed along the dashed line in Fig. 2(b). [1]

3. Kondo effect associated with singlet–triplet degeneracy

3.1. Effect of two-electron state degeneracy

Here we investigate Kondo effect in a quantum dot with even N, where the last two-electrons occupy a degenerate state consisting of a spin singlet and a spin triplet. The triplet consists of three degenerate two-electron states: $|S, S_z\rangle = |1, 1\rangle, |1, 0\rangle$ and $|1, -1\rangle$, where S_z is the z-component of the total spin on the dot. Suppose a co-tunneling process, starting from $|S, S_z\rangle = |1, 1\rangle$ in the triplet. Co-tunneling via a virtual state $|\frac{1}{2}, \frac{1}{2}\rangle$ can lead either to the triplet state $|1, 0\rangle$ or to the singlet state $|0, 0\rangle$. Via the second co-tunneling event, the state $|1, -1\rangle$ can be reached. As for the $S = 1$ case, the local spin can fluctuate by co-tunneling events. By coupling to all triplet states, the singlet state enhances the spin exchange interaction between the dot and leads, resulting in a strong Kondo effect, which is characterized by an enhanced T_K. Recent scaling calculations by Eto and Nazarov [25] indeed indicate a strong enhancement of T_K at the singlet–triplet degeneracy.

3.2. Experimental

The quantum dot used for the experiment on Kondo effect has a rectangular mesa (geometrical size: $0.45 \times 0.6\ \mu m^2$) and an internal confinement potential close to a 2D ellipse. The tunnel barriers between the dot and the external leads are thinner and lower than in the dot used in 2.2 such that co-tunneling processes are enhanced. Fig. 4(a) shows the linear response, dI/dV at $V = 0$ V vs. V_g and B. Regions shown in dark blue have low conductance, and correspond to the regimes

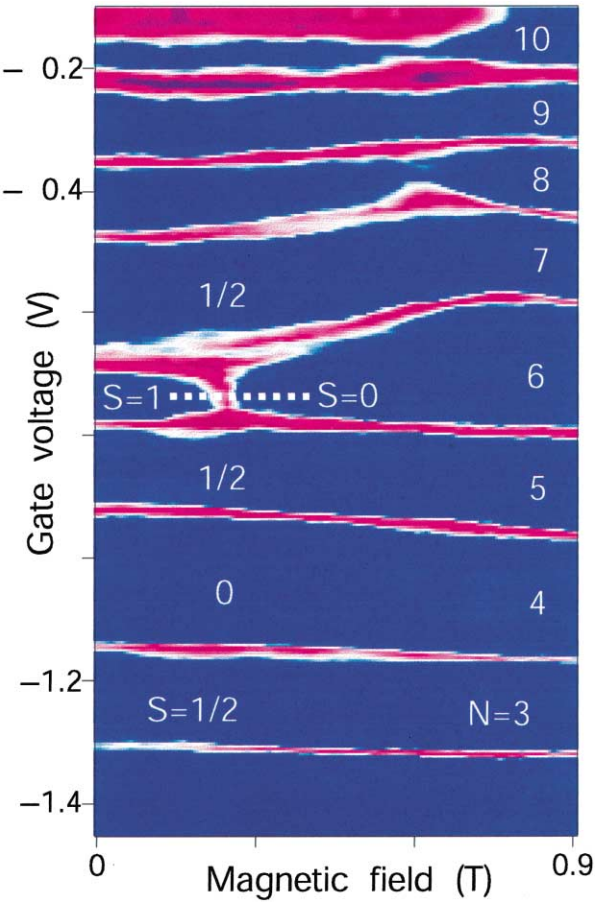

Fig. 4. Linear conductance vs. V_g and B measured at 14 mK. Dark blue regions of low conductance indicate Coulomb blockade. Red lines denote conductance peaks of height $\sim e^2/h$. The V_g position of the peaks reflects the ground state evolution with B, for $N = 3$–10.

of Coulomb blockade for $N = 3$–10. In contrast to previous experiments on the Kondo effect [9–12], all performed on lateral quantum dots with unknown electron number, here the number of confined electrons is precisely known. Red lines represent Coulomb peaks as high as $\approx e^2/h$. The pairing of the first two lower peaks reflects the GS evolution for $N = 3$ and 4, indicating the antiparallel filling of a same orbital for the third and fourth electrons. We find a modification to the pairing between the $N = 5$ and 6 GS lines. The $N = 5$ state has $S = \frac{1}{2}$, and the corresponding peak shows a smooth evolution with B. However, the $N = 6$ GS line has a small upward cusp at $B \approx 0.22$ T ($= B_0$). From earlier analyses [26] and from measurements

[1] There are various calculations consistent with our experiment; exact calculation for $N < 7$ is given in Refs. [17,18], Hartree–Fock calculations for $N > 8$ is given in Refs. [19–21], and spin density-functional theory at $B = 0$ T in Refs. [22,23] and also at non-zero B in Ref. [24].

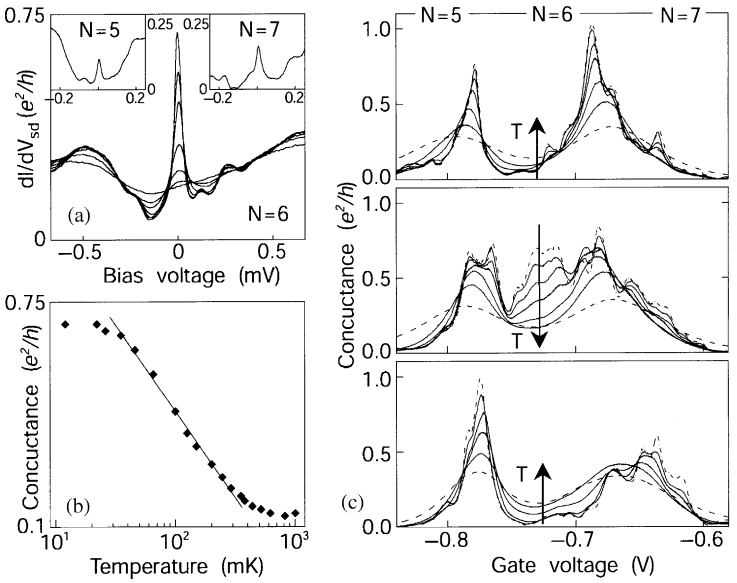

Fig. 5. Zero-bias resonance and T-dependence of the conductance at the singlet–triplet degeneracy. (a) Kondo resonance at the singlet–triplet transition. The dI/dV vs. V curves are taken at $V_g = -0.72$ V, $B = 0.21$ T and for $T = 14$, 65, 100, 200, 350, 520 and 810 mK. Insets to (a): Kondo resonances for $N = 5$ (left inset) and $N = 7$ (right inset), measured at $V_g = -0.835$ V and $V_g = -0.625$ V, respectively, and for $B = 0.11$ T and $T = 14$ mK. (b) Peak height of zero-bias Kondo resonance vs. T as obtained from (a) (filled diamonds). The solid line demonstrates a logarithmic T-dependence, which is characteristic of the Kondo effect. The saturation at low T is probably due to electronic noise. (c) T-dependence of the linear conductance vs. V_g for $B = 0.12$ T (spin-triplet ground state), $B = 0.22$ T (singlet–triplet degeneracy), and $B = 0.32$ T (spin–singlet ground state). Each panel shows 7 traces at $T = 20$ (dot–dashed line), 35, 70, 120, 260, 490 (solid lines) and 1050 (dashed line) mK. The arrows emphasize the temperature dependence in the valley for $N = 6$.

of the excitation spectrum (see Fig. 3) we can identify this cusp with a transition in the GS from a triplet to a singlet. At this transition we observe a strong enhancement of the conductance. In fact, over a narrow range around 0.22 T, the Coulomb gap for $N = 6$ disappears completely.

To explore this conductance anomaly, we show in Fig. 5(a) the data of dI/dV vs. V taken at $B = B_0$ and V_g corresponding to the dotted white line in Fig. 4. At temperature $T = 14$ mK, the narrow resonance around $V = 0$ V has a full-width at half-maximum, FWHM, of ≈ 30 μV. The height of the dI/dV peak resonance decreases logarithmically with T (Fig. 5(d)). These are typical 'fingerprints' of the Kondo effect. From FWHM ($=k_B T_K$), we estimate $T_K \approx 350$ mK. We note that we can safely neglect the Zeeman spin splitting because $g\mu B_0 = 5\ \mu\text{V} \ll k_B T_K$, implying that the spin triplet is in fact threefold degenerate at $B = B_0$. This condition is essential to the Kondo effect in the present study.

For $N = 6$, we find markedly anomalous T-dependence only at the singlet–triplet. Fig. 5(c) shows the dI/dV vs. V_g for different T. The upper panel shows data for $B = 0.12$ T. The two Coulomb peaks correspond to the transition from N=5–6 and from N=6–7. The small, short-period modulations superimposed on the Coulomb peaks are due to a weak charging effect in the upper part of the GaAs pillar above the dot. We will ignore this fine structure and focus on the general T-dependence. Upon increasing T, the valley conductance for $N = 6$ goes up due to thermally activated transport. A similar behavior is seen in the lower graph for $B = 0.32$ T. In contrast, at the single–triplet transition for $B = 0.22$ T we find an opposite T-dependence, again indicating the formation of a Kondo resonance. At the lowest T, the valley conductance is as high as $0.7e^2/h$, which is close to the height of the Coulomb peaks.

The T-dependence for $N = 5$ and 7 is visibly different from that in the non-Kondo valley for $N = 6$

(lower panel of Fig. 5(c)). Such a difference is a manifestation of the ordinary spin-$\frac{1}{2}$ Kondo effect expected for odd N. Indeed the corresponding zero-bias resonances are clearly observed (see insets to Fig. 5(a)). The height, however, is much smaller than for the singlet–triplet Kondo effect. There is also some indication for a triplet Kondo effect in the T-dependence for $N = 6$ at $B = 0.12$ T, although the associated zero-bias anomaly is not as apparent.

4. Conclusions

We have used two different vertical quantum dots to study the spin effects on the electronic properties. The first dot has a very weak coupling to the external leads. We use a magnetic field to adjust the single-particle state degeneracy, and observe parallel spin filling as favored by the direct Coulomb and exchange interactions at non-zero magnetic field. This means that electrons tend to have parallel spins in line with Hund's first rule when they occupy nearly degenerate single-particle states. The influence of the direct Coulomb and exchange interactions on the spin configurations is well explained in terms of two-electron singlet and triplet states. On the other hand, the tunnel barriers between the dot and the external leads are thinner and lower in the second dot than in the first dot such that co-tunneling processes are enhanced. In the same way as used for the first dot we adjust the single-particle state degeneracy as a function of magnetic field and observe a novel Kondo effect associated with the singlet–triplet degeneracy. In previous experiments Kondo effect is only observed when the quantum dot holds an odd number of electrons or a spin-half-state. In contrast our Kondo effect appears when the quantum dot holds an even number of electrons. The characteristic energy scale for this Kondo effect is much larger than in the ordinary spin-half-case.

Acknowledgements

We acknowledge the financial support from the Specially Promoted Research, Grant-in-Aid for Scientific Research and also from the Grant-in-Aid for Scientific Research on Priority Areas "Spin-Controlled Semiconductor Nanostructures" from the Ministry of Education, Science, Sports and Culture, Japan, from CREST-JST, from the Dutch Organization for Fundamental Research on Matter (FOM), and from the EU via a TMR network.

References

[1] B.L. Altshuler, P.A. Lee, R.A. Webb (Eds.), Mesoscopic Phenomena in Solids, Elsevier, Amsterdam, 1991.
[2] U. Meirav, E.B. Foxman, Semicond. Sci. Technol. 11 (1996) 255.
[3] L.L. Sohn, L.P. Kouwenhoven, G. Schoen (Eds.), Proceedings of the NATO Advance Study Institute on Mesoscopic Electron Transport, Kluwer, Dordrecht, Series E, Vol. 345, 105, 1997.
[4] S. Tarucha, D.G. Austing, T. Honda, R.J. van der Hage, L.P. Kouwenhoven, Phys. Rev. Lett. 77 (1996) 3613.
[5] S. Tarucha, T. Honda, D.G. Austing, Y. Tokura, K. Muraki, T.H. Oosterkamp, J.W. Janssen, L.P. Kouwenhoven, Physica E 3 (1998) 112.
[6] S. Tarucha, D.G. Austing, Y. Tokura, W.G. van der Wiel, L.P. Kouwenhoven, Phys. Rev. Lett. 84 (2000) 2425.
[7] L.I. Glazman, M.E. Raikh, JETP Lett. 47 (1998) 452.
[8] T.K. Ng, P.A. Lee, Phys. Rev. Lett. 61 (1988) 1768.
[9] D. Goldhaber-Gordon, Hadas Shtrikman, D. Mahalu, David Abusch-Magder, U. Meirav, M.A. Kastner, Nature 391 (1988) 156.
[10] S.H. Cronenwett, T.H. Oosterkamp, L.P. Kouwenhoven, Science 281 (1998) 540.
[11] J.R.H. Schimid, J. Weis, K. Eberl, K. Von Klitzing, Physica B 256 (1998) 182.
[12] F. Simmel, R.H. Blick, J.P. Kotthaus, W. Wegsheider, M. Bichler, Phys. Rev. Lett. 83 (1999) 804.
[13] S. Sasaki, S. De Franceschi, J.M. Elzerman, W.G. van der Wiel, M. Eto, S. Tarucha, L.P. Kouwenhoven, Nature 405 (2000) 764.
[14] V. Fock, Z. Phys. 47 (1928) 446.
[15] C.G. Darwin, Proc. Cambridge Philos. Soc. 27 (1930) 86.
[16] L.P. Kouwenhoven, T.H. Oosterkamp, M.W.S. Danoesastro, M. Eto, D.G. Austing, T. Honda, S. Tarucha, Science 278 (1997) 1788.
[17] A. Wojs, P. Hawrylak, Phys. Rev. B 53 (1996) 10 841.
[18] M. Eto, Jpn. J. Appl. Phys. 36 (1997) 3924.
[19] A. Natori et al., Jpn. J. Appl. Phys. 36 (1997) 3960.
[20] H. Tamura, Physica B 249–251 (1998) 210.
[21] M. Rontani et al., Phys. Rev. B 59 (1999) 10 165.
[22] In-Ho Lee et al., Phys. Rev. B 57 (1998) 9035.
[23] M. Koskinen, M. Manninen, S.M. Reimann, Phys. Rev. Lett. 79 (1997) 1817.
[24] O. Steffen, U. Rossler, M. Suhrke, Europhys. Lett. 42 (1998) 529.
[25] M. Eto, Yu. Nazarov, Phys. Rev. Lett. 85 (2000) 1306.
[26] D.G. Austing, S. Sasaki, S. Tarucha, S.M. Reimann, M. Koskinen, M. Manninen, Phys. Rev. B 60 (1999) 11 514.